Modeling and simulation of fracture and fragmentation

M. Ortiz
California Institute of Technology

11th World Congress on Computational Mechanics (WCCM XI)
July 22, 2014, Barcelona, Spain

Fracture as engineering design limiter

- Fracture and fragmentation occur under a variety of conditions (static, dynamic, fatigue, ductile, corrosion...), *set limits on engineering designs*
- Fracture is the result of mechanisms that play out across disparate spatial and time scales, from atomistic to continuum (*multiscale phenomena*)
- Fracture leads to, possibly time-dependent, displacement discontinuities that challenge approximation schemes (*free discontinuities*)
- Fracture processes, crack patterns, can exhibit great *complexity*, *stochasticity*, *uncertainty*, *coupling to environment*, which adds to challenge

The range of fracture mechanics…

Quasistatic fatigue crack growth: Mostly LEFM, also corrosion-fatigue cracking...

Detail of cabin window crack of a de Havilland Comet G-ALYP recovered from the Mediterranean after its crash in January 1954 (http://www.ssplprints.com)

Aloha Airlines flight 243 ‘blows its top’ on April 28, 1988. Failure attributed to fatigue cracks nucleated at rivet holes through environmentally-assisted cracking

The range of fracture mechanics…

Environmentally assisted cracking: Brittle/ductile transition, stress-corrosion cracking...

Liberty ship split in half on reaching the ductile-to-brittle transition temperature (Photograph courtesy of the Principle and Fellows of Newnham College, Cambridge)

Failure of the New Carissa, on February 3, 1999, as a result of stress-corrosion cracking caused by extreme heat from burning, cyclic bending and seawater.

The range of fracture mechanics…

Dynamic fracture and fragmentation: Complexity, stochastic behavior, extreme material behavior...

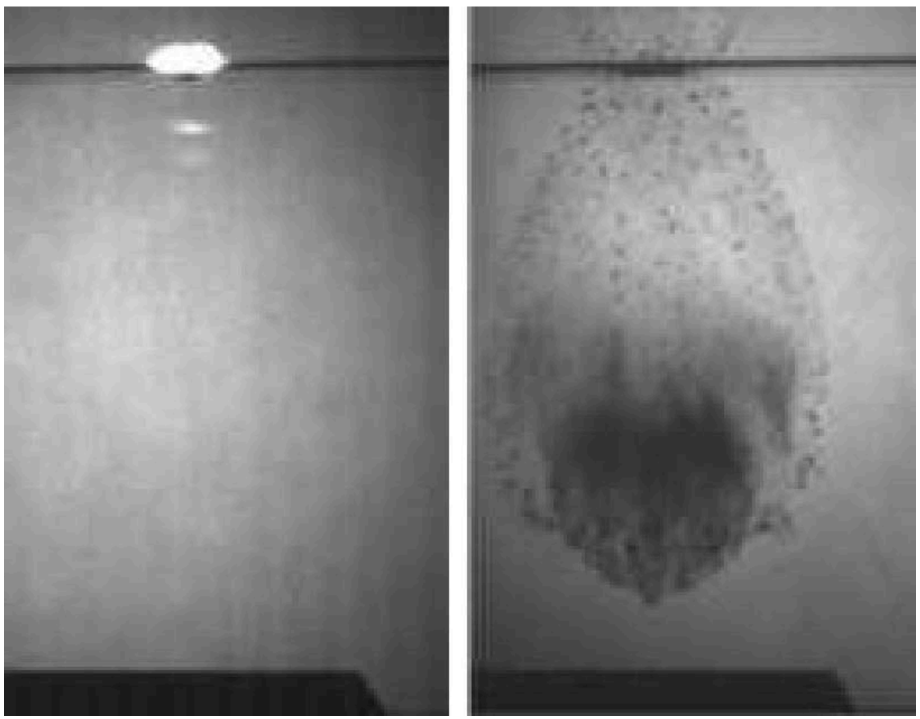

Hypervelocity impact of bumper shield. a) Initial impact flash. b) Debris cloud (Ernst-Mach Inst., Freiburg, Germany).

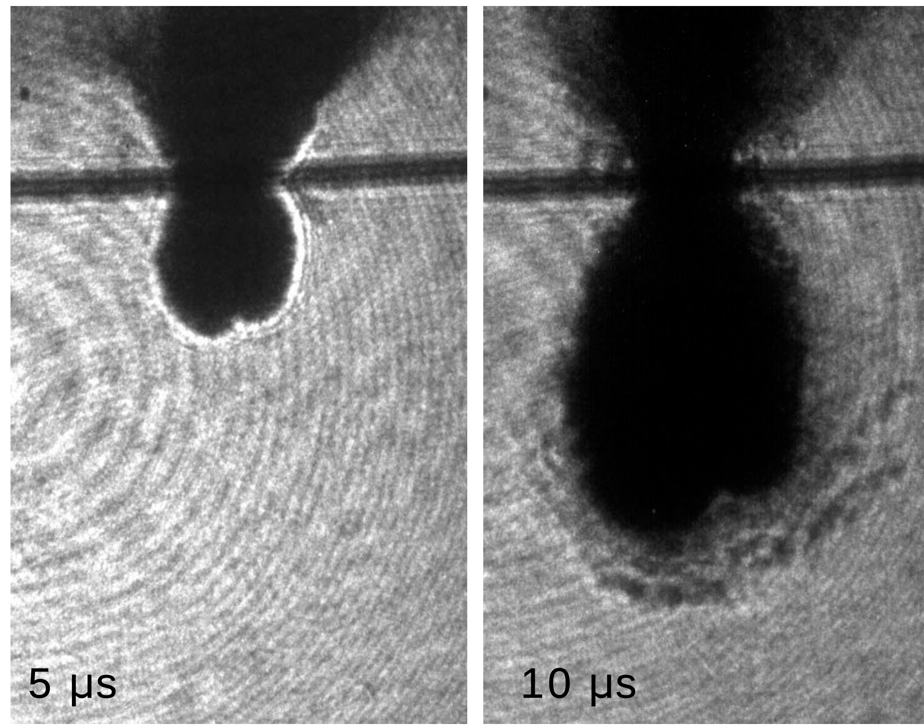

Hypervelocity impact (5.7 Km/s) of 0.96 mm thick aluminum plates by 5.5 mg nylon 6/6 cylinders (Caltech)

The range of fracture mechanics…

Hydraulic fracture: Example of extreme complexity, uncertainty, coupling to the environment…

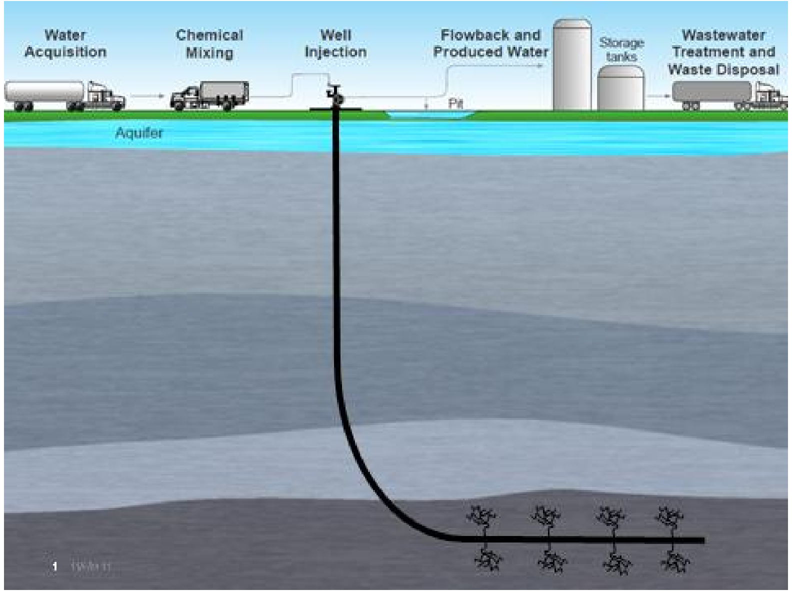

Schematic of hydraulic fracture by horizontal drilling (S. Green and R. Suarez-Rivera, AAPG Geoscience Technology Workshop, 2013)

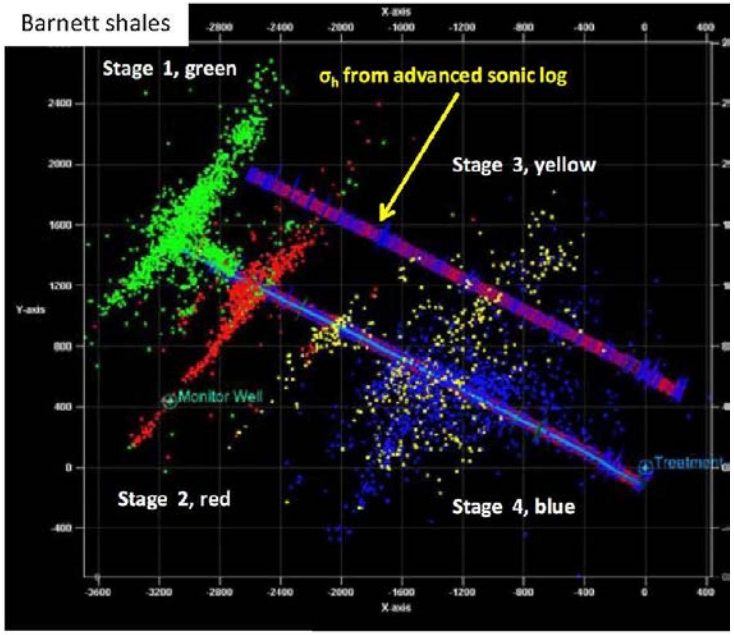

Complex pattern of hydraulic fractures generated during fracking mapped from acoustic emissions (R. Wu *et al*., SPE-152052-MS, 2012)

Modeling & simulation desiderata

- Numerical schemes must ideally be:
  - *Capable of handling geometrical and topological* ***complexity*** *in the crack set and its evolution*
  - ***Agnostic as regards material behavior****, i.e., they must apply equally well regardless of whether the material:*
    - *Is elastic or inelastic (e.g., plastic, viscoelastic…)*
    - *Undergoes small or large deformations*
    - *Deforms quasistatically or dynamically*
  - *Defined in terms of material constants measurable by means of* ***standard fracture tests*** *(e.g., ASTM standards)*
  - ***Provably convergent****, including crack set, with respect to mesh and time-step refinement (****verification****)*
  - ***Predictive*** *of crack initiation and growth under relevant conditions of loading, temp., environment (****validation****)*

Fracture as a free-discontinuity problem

- ***How do we 'mathematize' fracture?***
- ***What is the problem to be solved?***
- Deformation mapping discontinuous!
  - Jump set $J(\varphi) \subset C \equiv$ crack set
  - $D\varphi$ integrable in $B \backslash C$
- Functional framework: SBV[1,2] ...
- Elastic energy: For φ injective,

$$E(t, \underline{\varphi, C}) = \int_{B \backslash C} W(\nabla \varphi)\, dx + \text{forcing terms}$$

equilibrium + crack tracking!

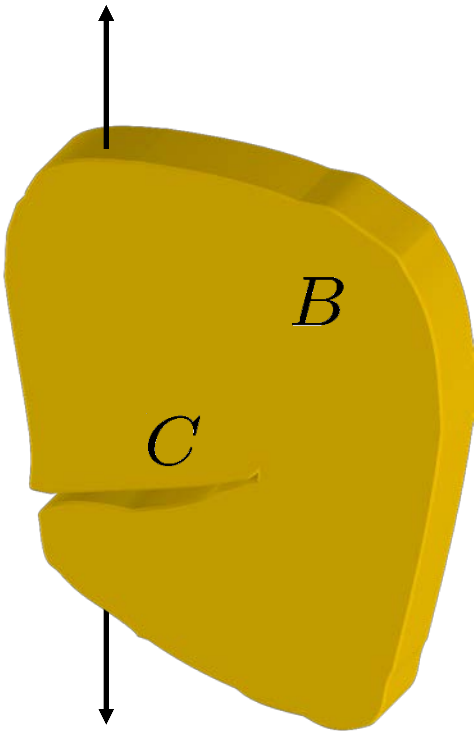

[1]Ambrosio, L., *Boll. Un. Mat. Ital. B*, **3** (1989) 857.
[2]Francfort, G. A. and Marigo, J. J., *JMPS*, **46** (1998) 1319.

Fracture as a dissipative process

- Fracture is an irreversible process!
- Griffith[1]: Rate indep., no R-curve
- Dissipation: $D(C_1, C_2) =$

$$\begin{cases} G_c |C_2 \setminus C_1|, & C_1 \subset C_2, \\ +\infty, & \text{otherwise.} \end{cases}$$

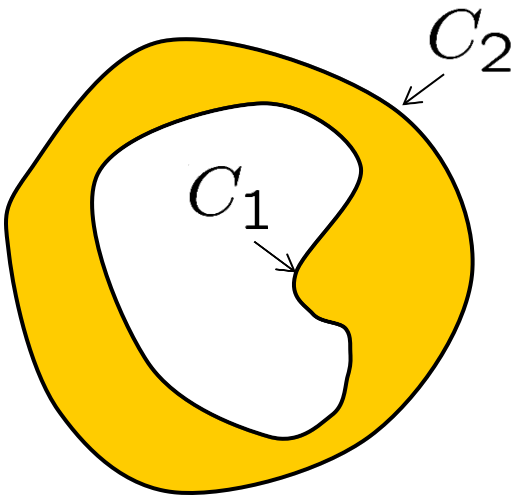

- Energetic solutions[2]: Stability + energy balance,

$$E(t, \varphi(t), C(t)) - E(t, \varphi'(t), C'(t)) \leq D(C(t), C'(t))$$

$$\int_0^t \partial_t E(s)\, ds = E(t) - E(0) + D(C(0), C(t))$$

[1]Griffith, A., *Philos. Trans. Roy. Soc. London, Ser. A*, **221** (1921) 163.
[2]A. Mielke & Theil, F., *NoDEA Nonlinear Diff. Eq. Appl.*, **11** (2004) 151.

Fracture as a dissipative process

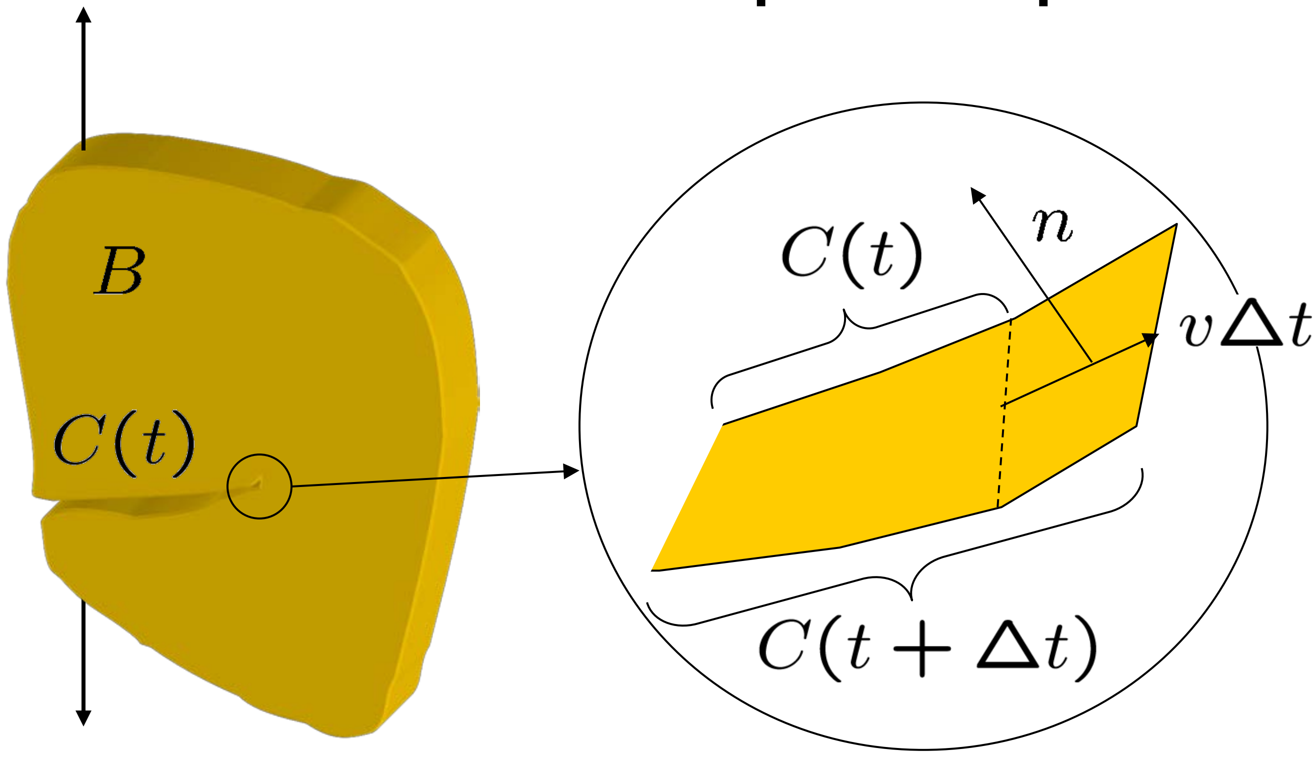

- Along smooth solutions: $-\dot{E} = \int_{\partial C} G(s)v(s)\,ds$
- Griffith criteria[1]: $G - G_c \leq 0, \quad v \geq 0, \quad (G - G_c)v = 0$

[1]Griffith, A., *Philos. Trans. Roy. Soc. London, Ser. A*, **221** (1921) 163.

Michael Ortiz
WCCM XI

Time discretization of energetic solutions

- Discretize time: $t_0, \dots, t_n, t_{n+1} + \Delta t \dots$
- Time-discretized variational solutions[1]:

$$E(t_{n+1}, \varphi_{n+1}, C_{n+1}) - E_n + D(C_n, C_{n+1}) \to \text{inf!}$$

- Extension to inelasticity[1]: $E_{n\to n+1}(\varphi_{n+1}, C_{n+1})$

$$= \int_{B\backslash C_{n+1}} W_{n\to n+1}(\nabla\varphi_{n+1})\, dx + \text{forcing terms}$$

$$\Rightarrow E_{n\to n+1}(\varphi_{n+1}, C_{n+1}) + D(C_n, C_{n+1}) \to \text{inf!}$$

- Dynamics[2]: $\int_B (\rho_0/2\Delta t)|\varphi_{n+1} - \varphi_{n+1}^{\text{pred}}|^2\, dx$

$$+ E_{n\to n+1}(\varphi_{n+1}, C_{n+1}) + D(C_n, C_{n+1}) \to \text{inf!}$$

[1] Ortiz, M. & Stainier, L., *CMAME*, **171** (1999) 419.
[2] Radovitzky, R. & Ortiz, M., *CMAME*, **172** (1999) 203.

Computational fracture: The essential difficulty…

- Time-discretized variational principles deliver *energetic solutions* to the fracture problem, including crack tracking, inelasticity and inertia
- *The essential difficulty*: Efficient representation of *complex evolving surfaces*, including kinking (non-smoothness) branching (non-manifold) and fragmentation (topological transitions)
- *Interfacial/cohesive elements*: Static, dynamic, material-agnostic, but convergence requires mesh adaption[2] (ability to span all meshes)
- Alternative paradigm[1]: *Regularization!* (e.g., non-local damage, phase-field models…)

[1]Ambrosio, L. & Tortorelli, V. M., *Comm. Pure Appl. Math.*, **43** (1990) 999.
[2]Fraternali, F., Negri, M. & Ortiz, M., *Int. J. Fract.*, **166** (2010) 3.

Eigenfracture: Fracture *via* eigenstrains

- Regard fracture as an energy-relaxation process!
- Total incremental energy[1]: Elastic + fracture,

$$E_\epsilon(u,e^*) = \int_\Omega W(e(u) - e^*)\,dx + \frac{G_c}{2\epsilon}|\{e^* \neq 0\}_\epsilon|$$

eigenstrains!

$C \equiv \{e^* \neq 0\}$

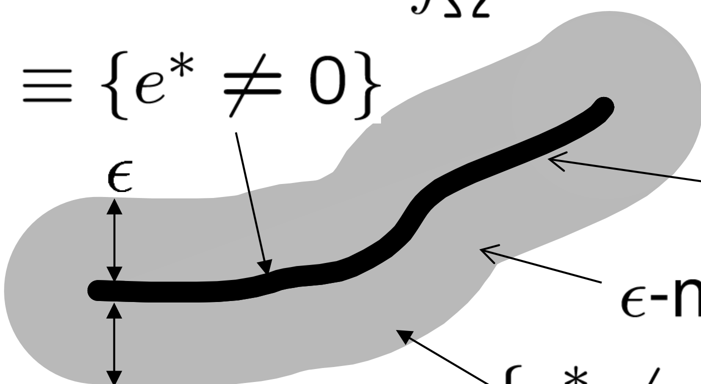

- Energy-minimizing cracks: $E_\epsilon(u,e^*) \to \inf$!
- <u>**Theorem**</u>[1]: $\Gamma - \lim_{\epsilon\to 0} E_\epsilon =$ Griffith energy

[1]Schmidt, B., *et al.*, *SIAM Multi. Model.*, **7** (2009) 1237.

Eigenfracture: Spatial discretization

- Spatial discretization:

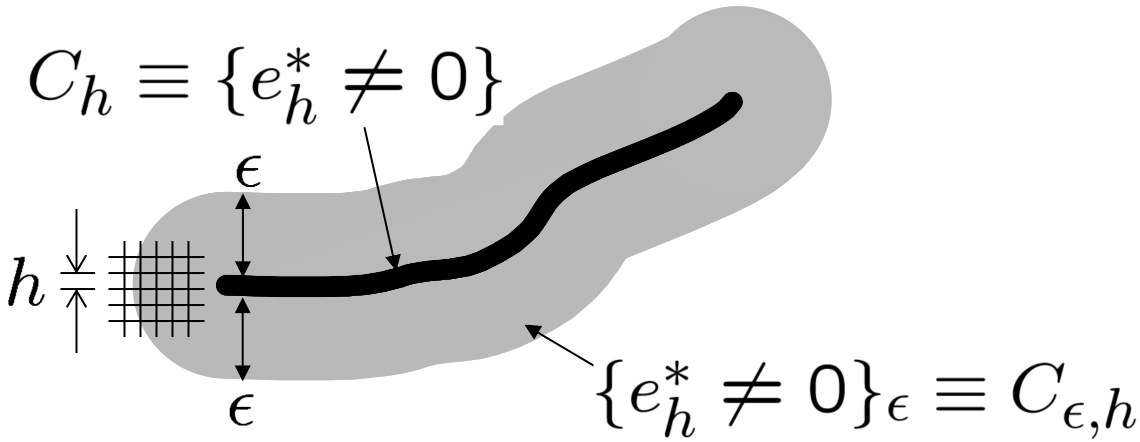

- Discretized incremental energy:

$$E_{\epsilon,h}(u,e^*) = \begin{cases} E_\epsilon(u,e^*), & \text{if } u \in V_h,\ e^* \in W_h, \\ +\infty, & \text{otherwise.} \end{cases}$$

- **Theorem**[1]: Suppose $\epsilon = \epsilon(h)$ and $h/\epsilon(h) \to 0$ as $h \to 0$. Then, $\Gamma - \lim_{h\to 0} E_{h,\epsilon(h)} =$ Griffith energy

[1]Schmidt, B., *et al.*, *SIAM Multi. Model.*, **7** (2009) 1237.

Eigenerosion: Erosion *via* eigenfracture

- For every element K, choose[1,2]
  - either: $e^*_K = e(u_K) \Rightarrow$ element erosion,
  - or: $e^*_K = 0 \Rightarrow$ intact element.
- Erosion criterion: $-\Delta E_K \geq \frac{G_c}{2\epsilon} \underbrace{|(C \subset K)_\epsilon \backslash C_\epsilon|}$

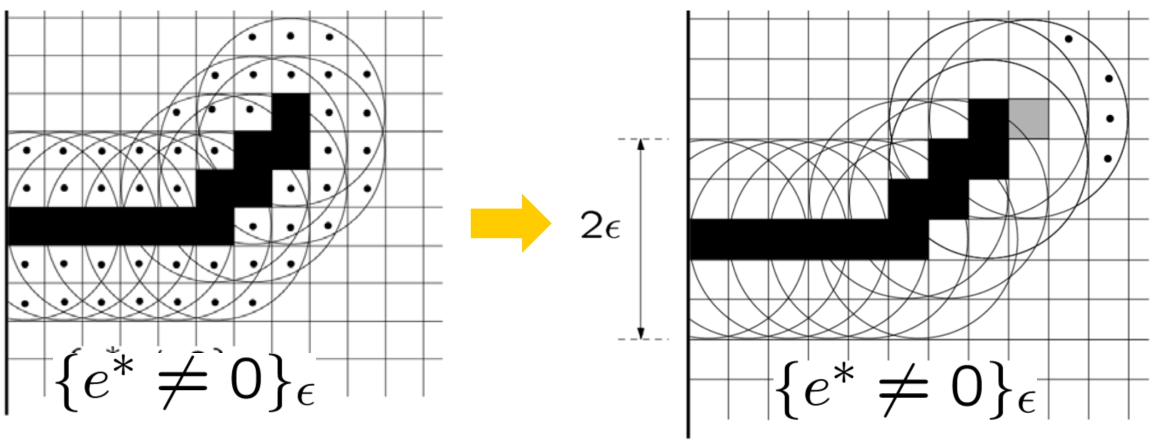

- To first order[1,2]: $-\Delta E_K \sim$ energy in element K

[1]Pandolfi, A. & Ortiz, M. , *IJNME*, **92** *(*2012) 694.
[2]Pandolfi, A., Li, B. & Ortiz, M. , *Int. J. Fract.*, **184** *(*2013) 3.

Eigenerosion — Flow chart

(i) **Set** time to t_{n+1}, **initialize** crack set $C_{n+1}=C_n$

(ii) **compute** predictor fields

(iii) **compute** equilibrium fields

(iv) **for** every element K **do**:
compute net energy release: $-\Delta E_K - G_c \Delta A_K$
if > 0, **insert** in priority queue *PQ*

(v) **if** $PQ \neq \emptyset$, **pop** *PQ*, **insert** in C_{n+1}, **goto** (ii)
otherwise compute updated fields, **exit**

Verification – Mode-I edge-crack panel

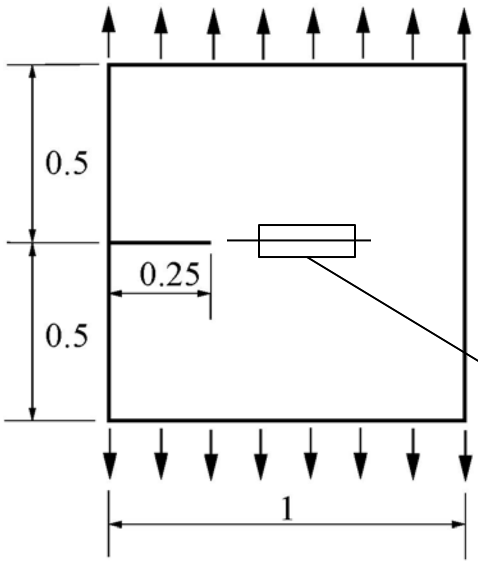

- Mesh slanted at 20° to crack plane
- ε-construction compensates for slant and tracks the exact crack path *on average*

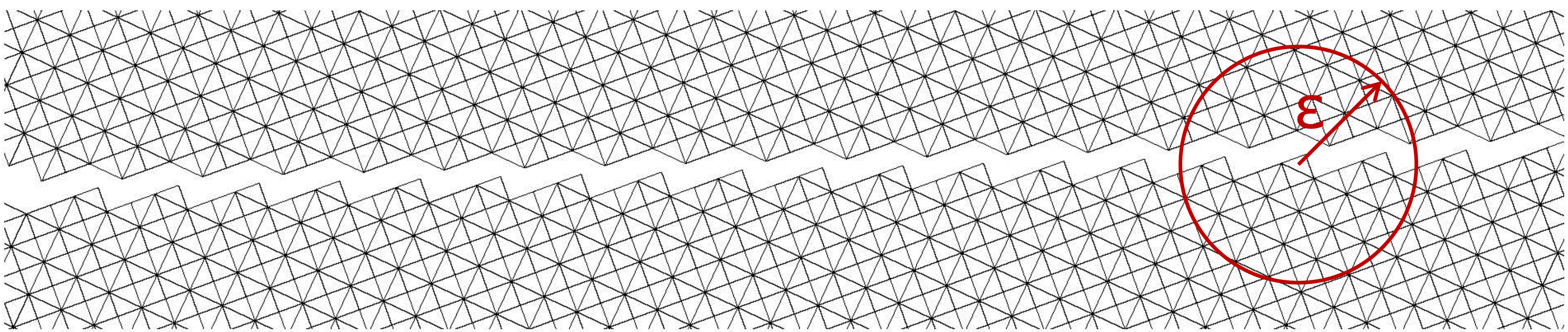

Pandolfi, A. and Ortiz, M., *IJNME*, **92** (2012) 694.

Verification – Mode-I edge-crack panel

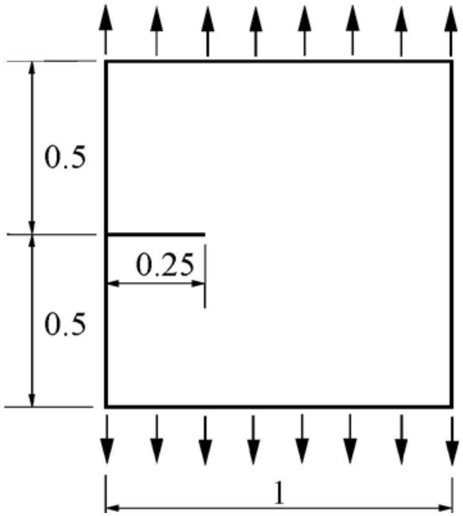

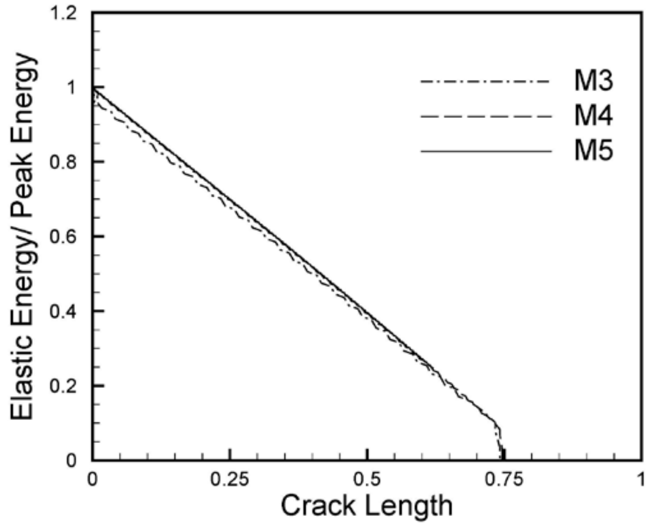

- Random mesh:
  - Convergence
  - Mesh insensitive
  - Good accuracy

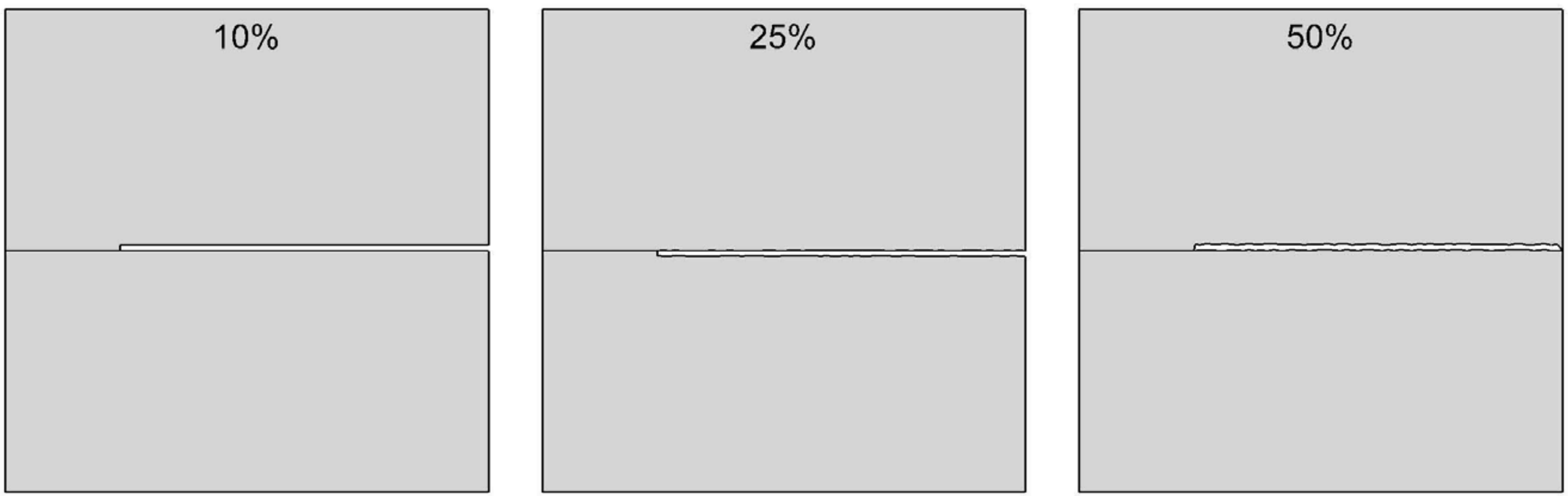

Pandolfi, A. and Ortiz, M., *IJNME*, **92** (2012) 694.

Verification: Mode I-III 3-point bending

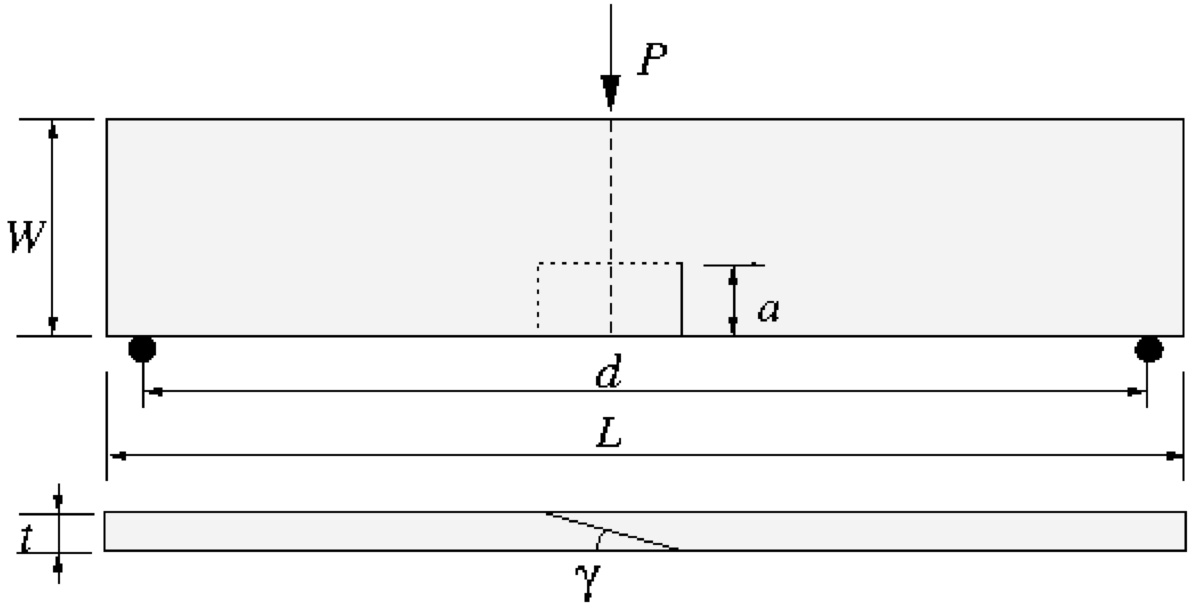

- Mixed-mode 3-point bending tests, PMMA plates (260x60x10 mm, a = 20 mm)
- Inclination of notch: 75°, 60°, 45°
- E = 2800 MPa, n = 0.38, G_c = 0.54 N/mm

Lazarus, V. *et al.*, *Int. J. Fract.*, **153** (2008) 141.

Predominant Mode III (γ = 45°)

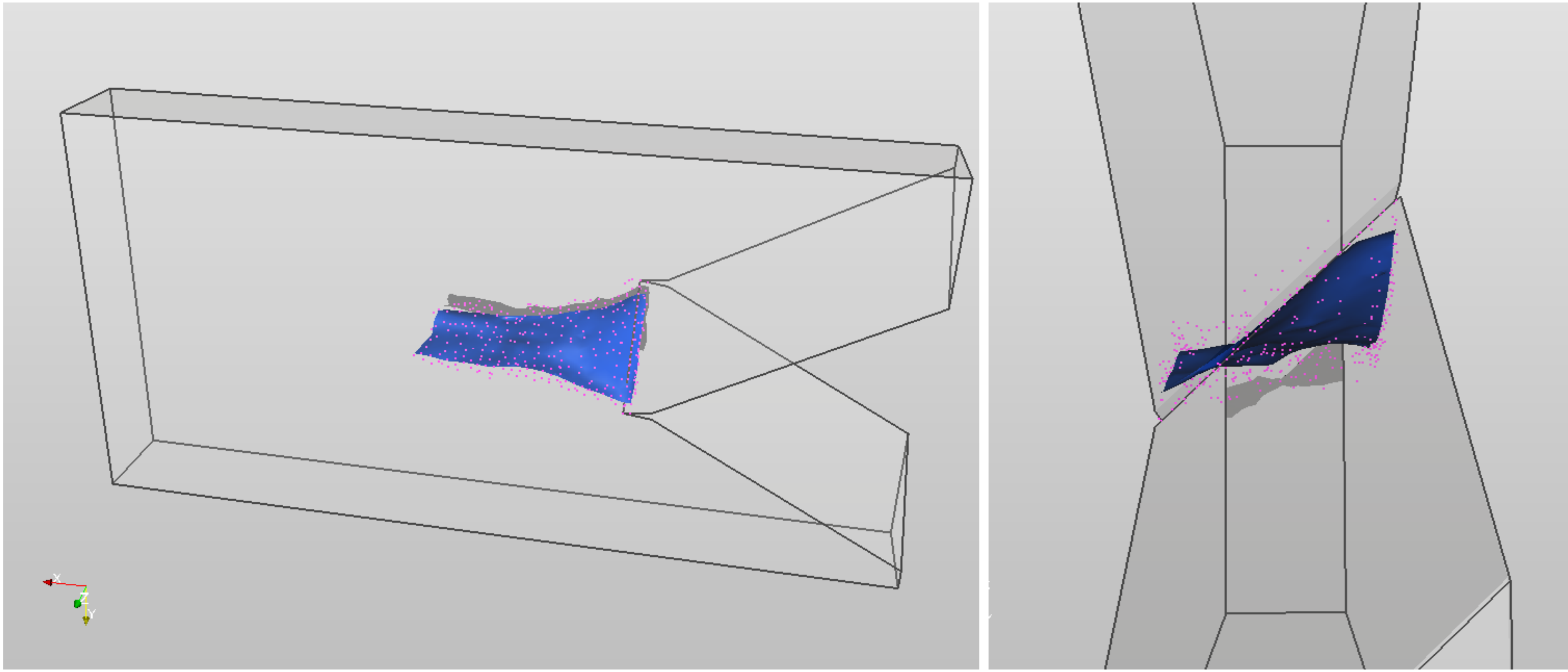

Mixed mode I-III crack growth in three-point bending

Pandolfi, A. & Ortiz, M., *IJNME*, **92** (2012) 694.

Verification: Mode I-III 3-point bending

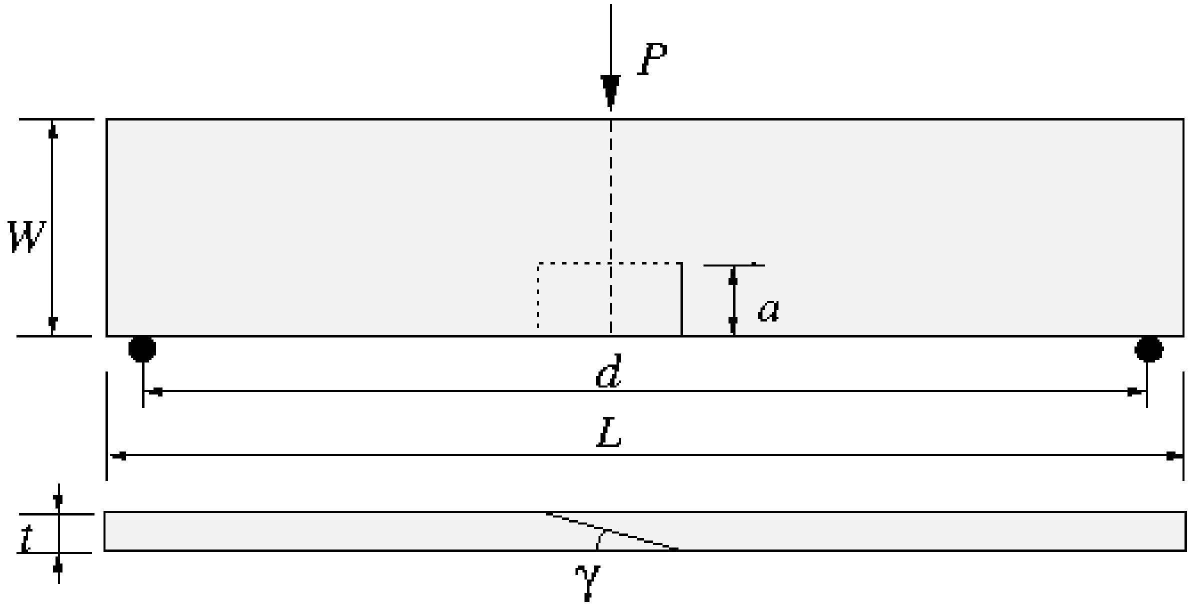

γ	α Lazarus et al. [2008]	α_R	α_L	α	error %
75	21.1	22	18	20.0	5.1
60	38.4	36	35	35.5	7.6
45	61.9	57	58	57.5	7.1

Lazarus, V. *et al.*, *Int. J. Fract.*, **153** (2008) 141.
Pandolfi, A. & Ortiz, M., *IJNME*, **92** (2012) 694.

Mixed Mode I–III Al_2O_3 Rod Experiments

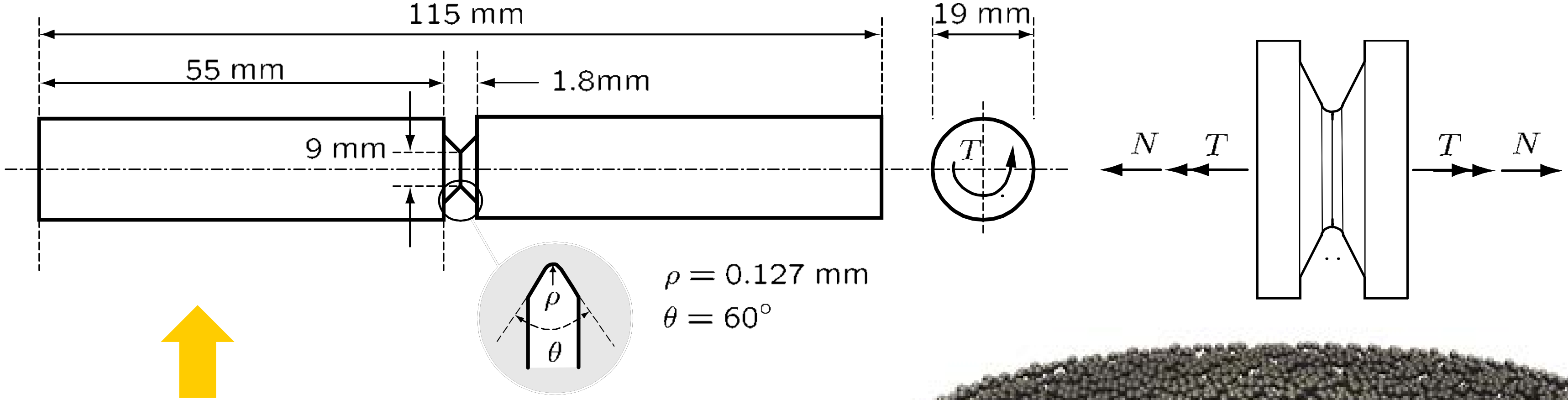

Circumferentially-notched Al_2O_3 cylindrical rods tested under combined tension and torsion[1].

Mesh-free computational model of 104K nodes and 514K material particles[2].

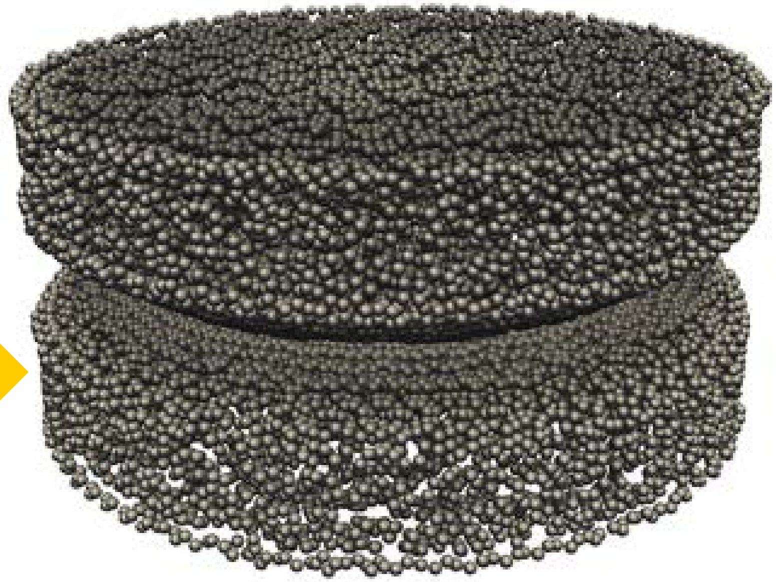

[1]Suresh, S. & Tschegg, E. K., *J. Am. Ceram. Soc.*, **70** (1987) 726.
[2]Pandolfi, A., Li, B. & Ortiz, M., *Int. J. Fract.*, **184** (2013) 3.

Al_2O_3 Rod – Pure Torsion

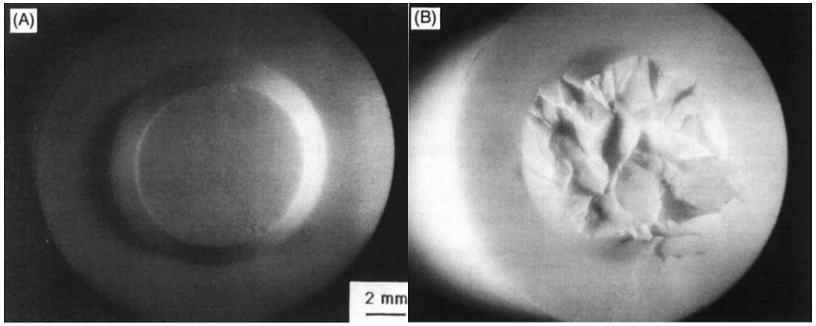

Observed fractography[1]

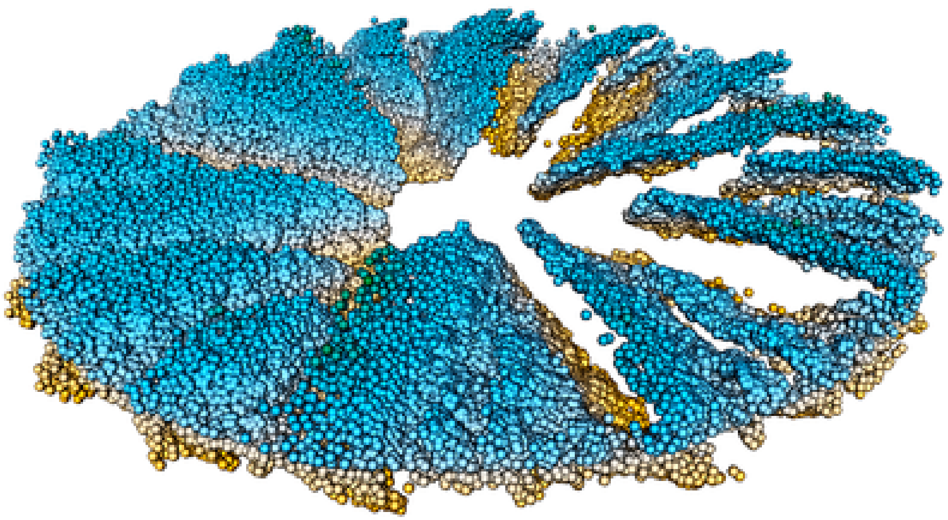

Failed material-point set[2]

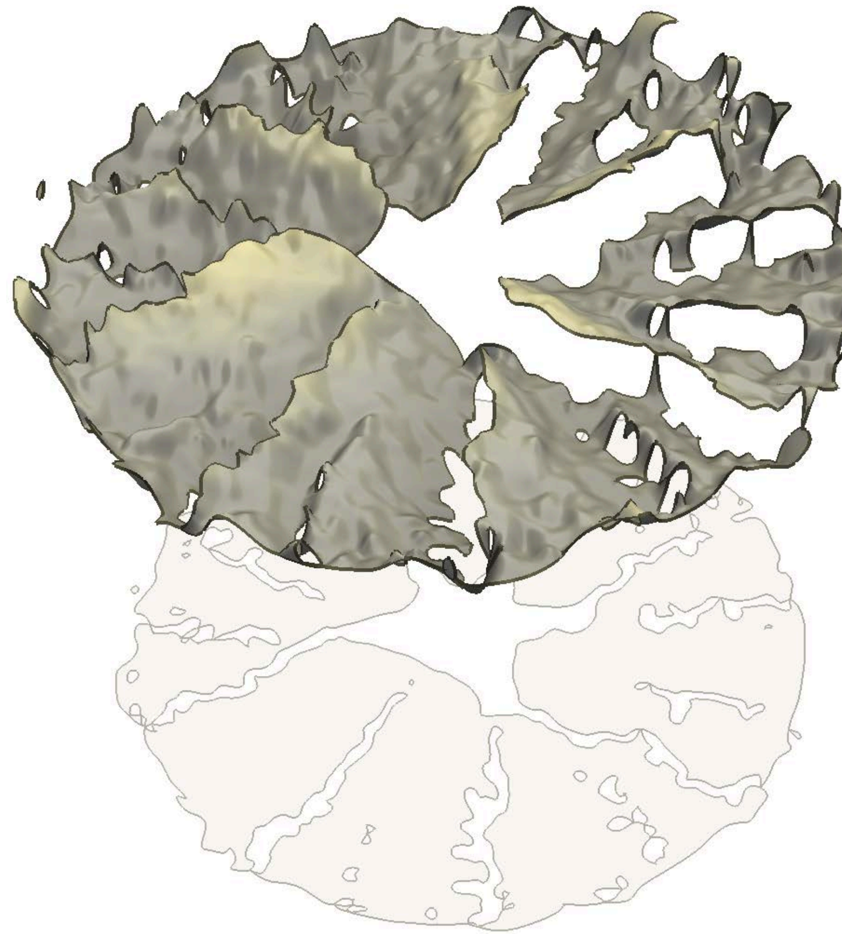

Reconstructed crack surface[2]

[1]Suresh, S. & Tschegg, E. K., *J. Am. Ceram. Soc.*, **70** (1987) 726.
[2]Pandolfi, A., Li, B. & Ortiz, M., *Int. J. Fract.*, **184** (2013) 3.

Validation – Explosively driven cap

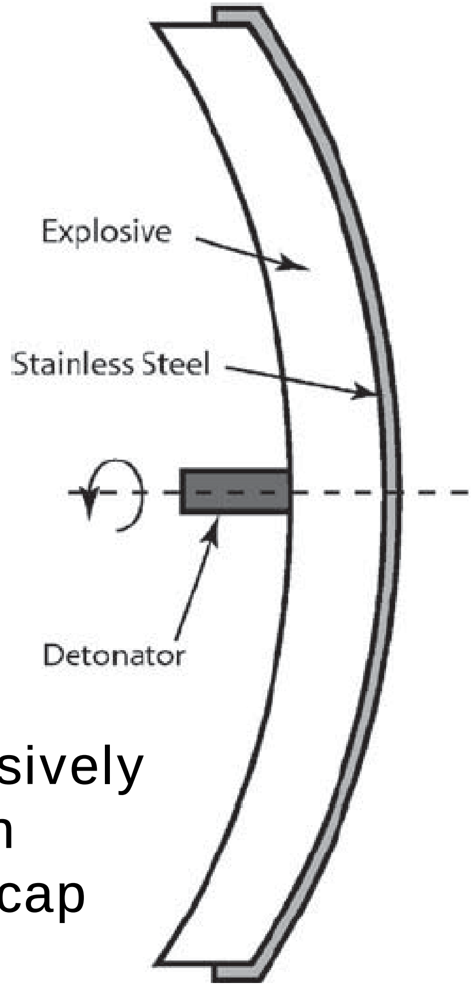

Explosively driven steel cap

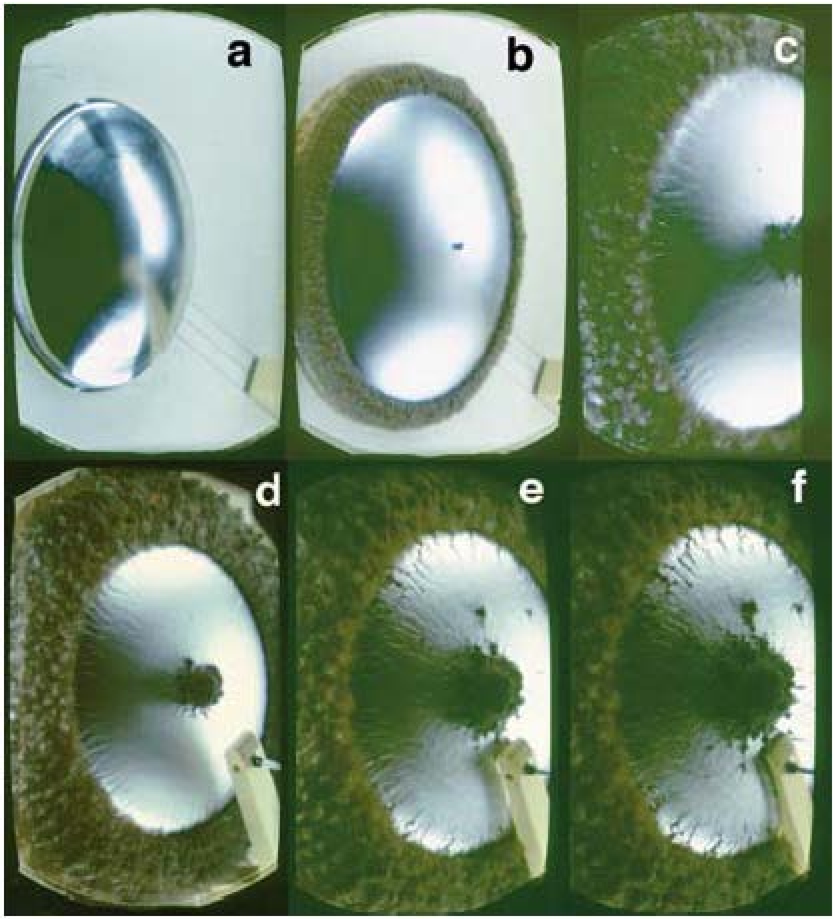

Optical framing camera records

G.H. Campbell *et al*., *JAP*, **101** (2007) 033540.

Validation – Explosively driven cap

Experiment

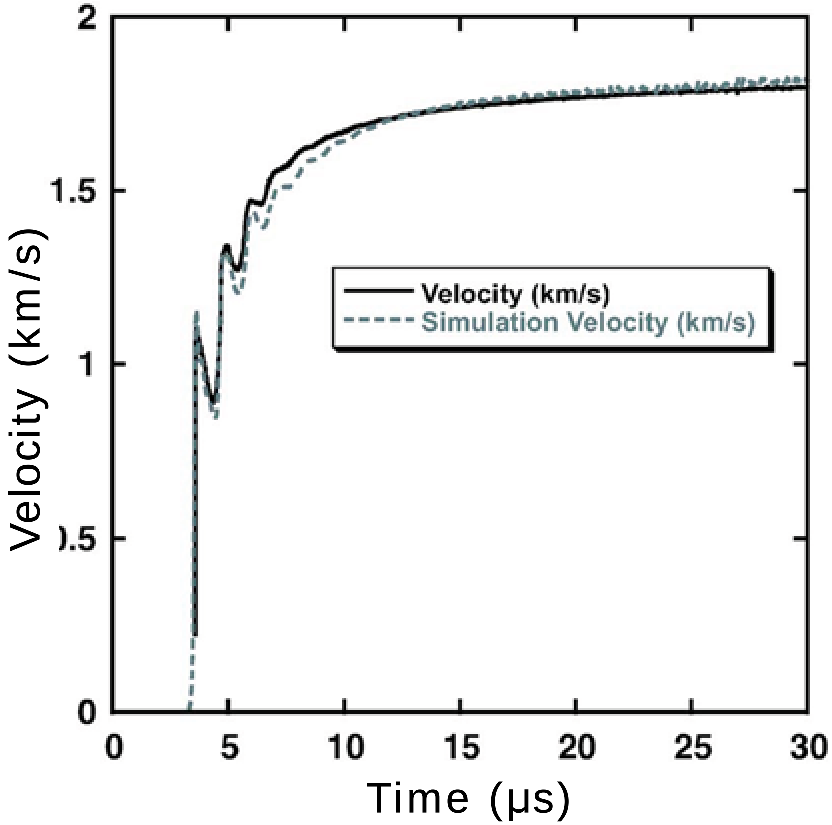

OTM simulation

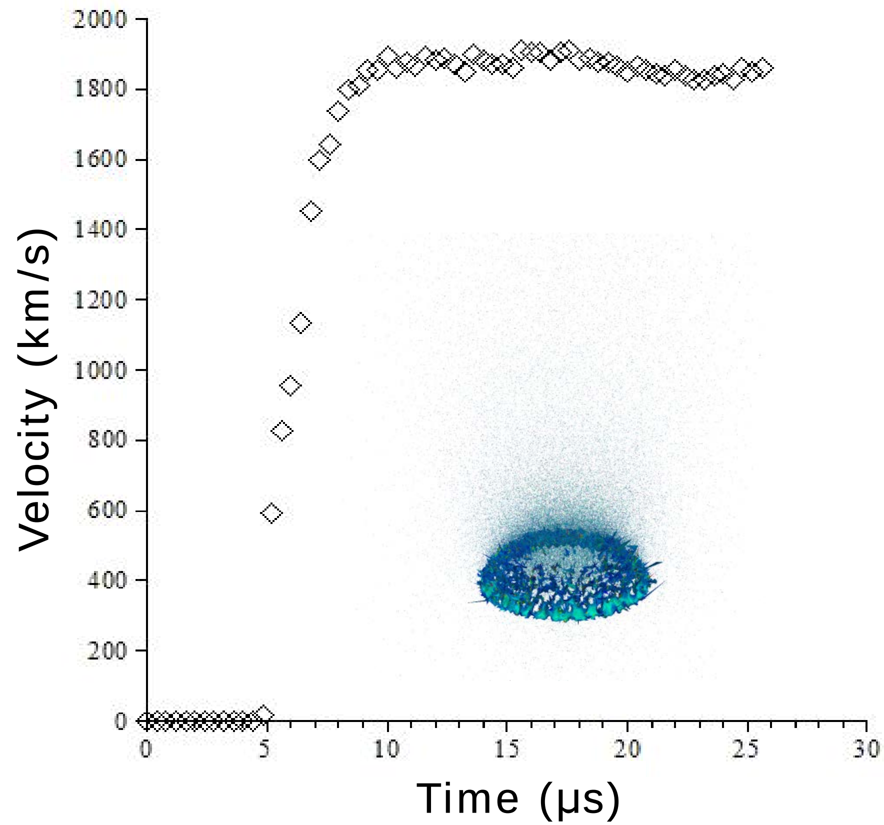

Surface velocity for spot midway between pole and edge

Campbell, G. H. *et al.*, *JAP*, **101** (2007) 033540.
Li, B., Pandolfi, A. & Ortiz, M., *Mech. Mater*. (2014) in press.

Validation – Explosively driven cap

Experiment

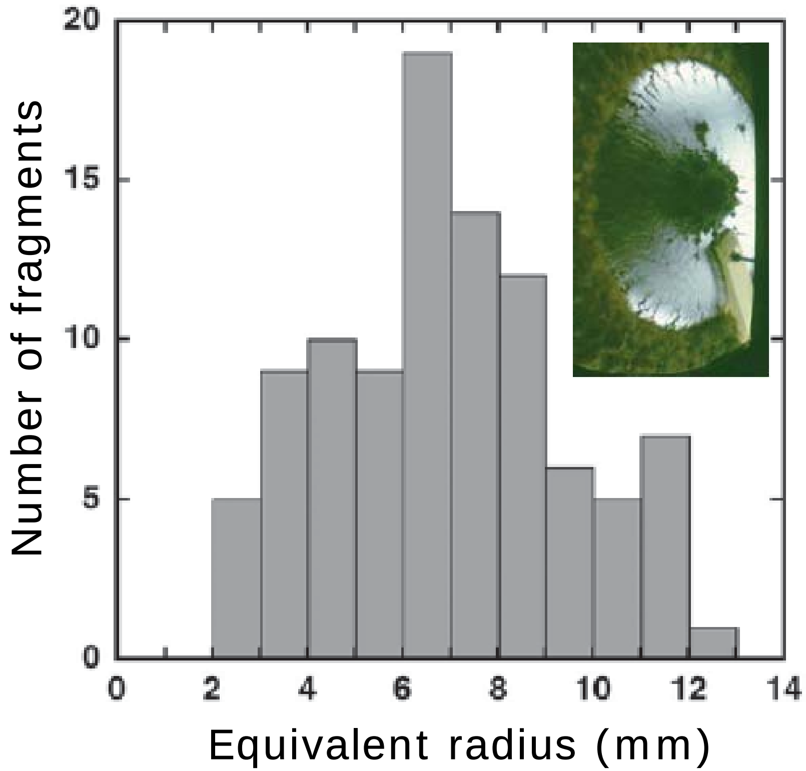

OTM simulation

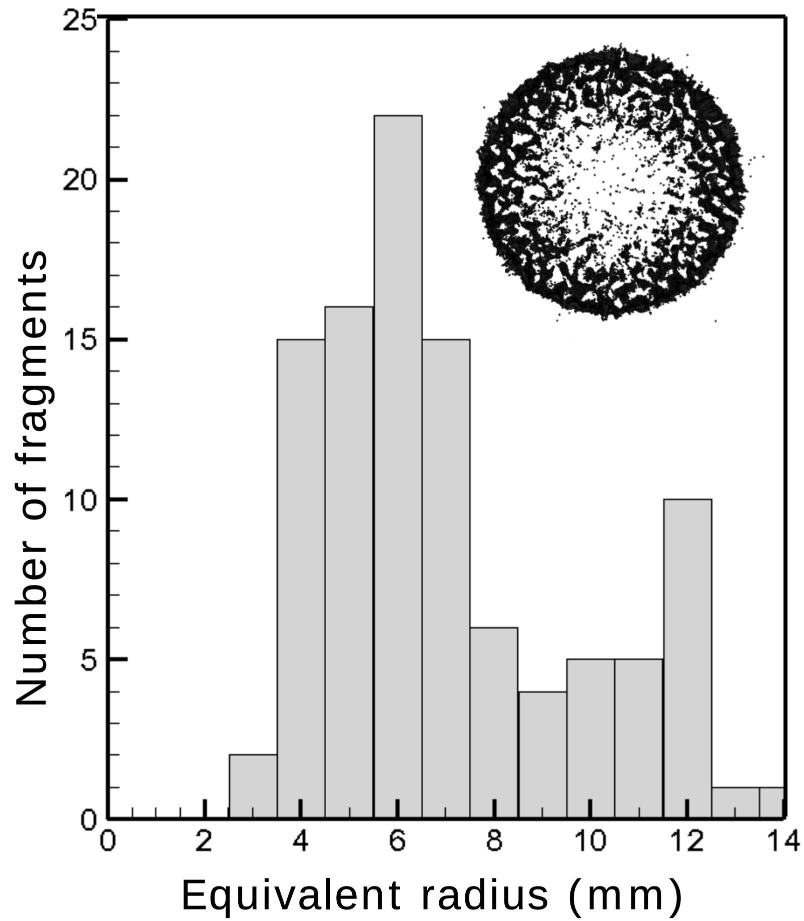

Histograms of equivalent fragment radii

Campbell, G. H. *et al.*, *JAP*, **101** (2007) 033540.
Li, B., Pandolfi, A. & Ortiz, M., *Mech. Mater*. (2014) in press.

Michael Ortiz
WCCM XI

Validation – Failure waves in glass rods

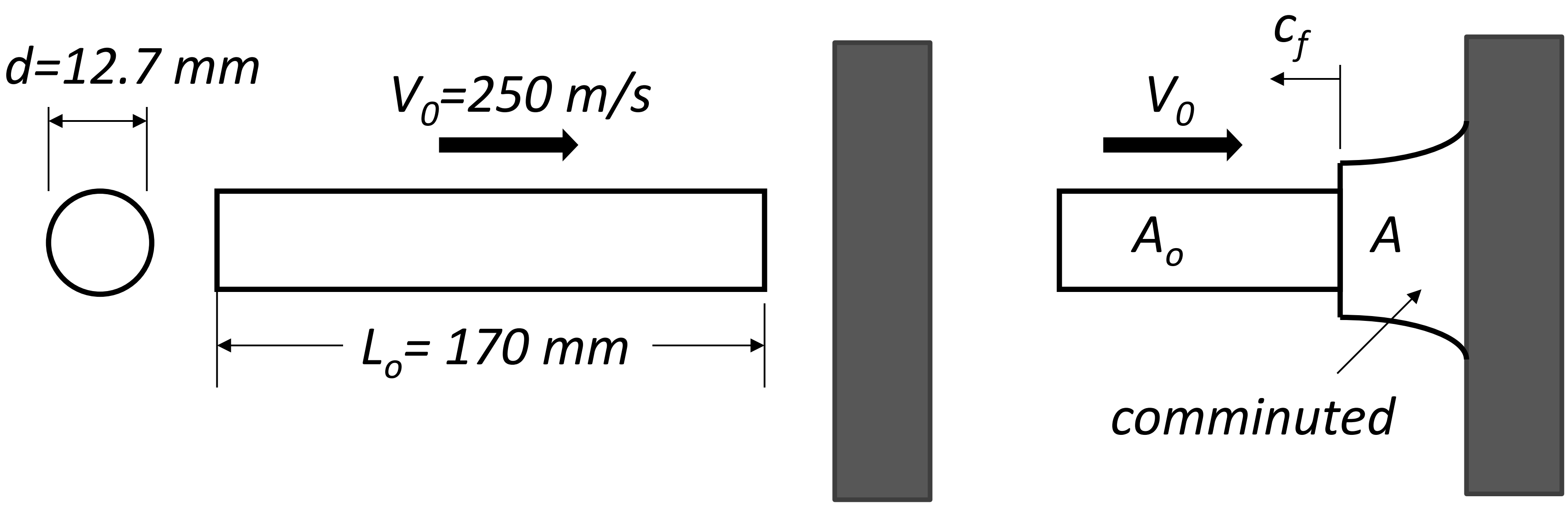

- V_0=225 m/s, c_f = 3.6 Km/s (Brar & Bless, 1991)
- V_0=250 m/s, c_f = 3.0 Km/s (Repetto *et al.*, 2000)

Brar, N.S. & Bless, S.J., *Appl. Phys. Let.*, **59 (**1991) 3396.
Repetto, E.A. *et al.*, *CMAME*, **183** (2000) 3.

Application to hypervelocity impact

Caltech's hypervelocity Impact facility

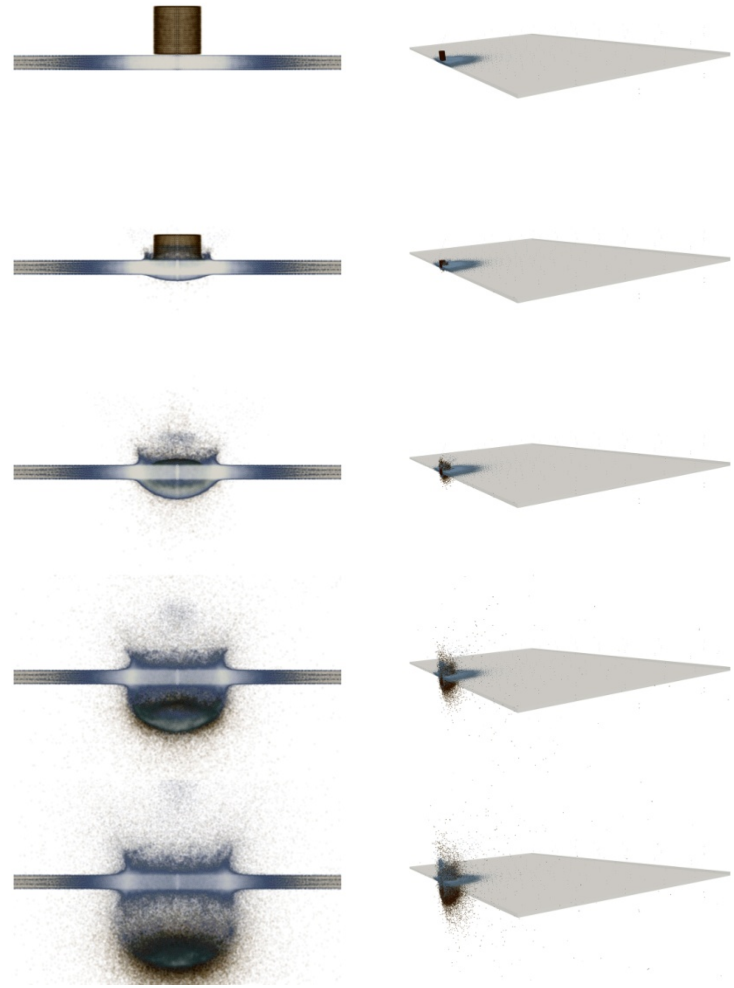

OTM simulation, 5.2 Km/s, Nylon/Al6061-T6

Li, B., Stalzer, M. & Ortiz, M., *IJNME* (2014) in press.

Application to hypervelocity impact

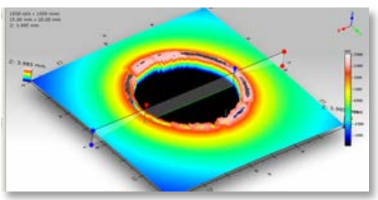

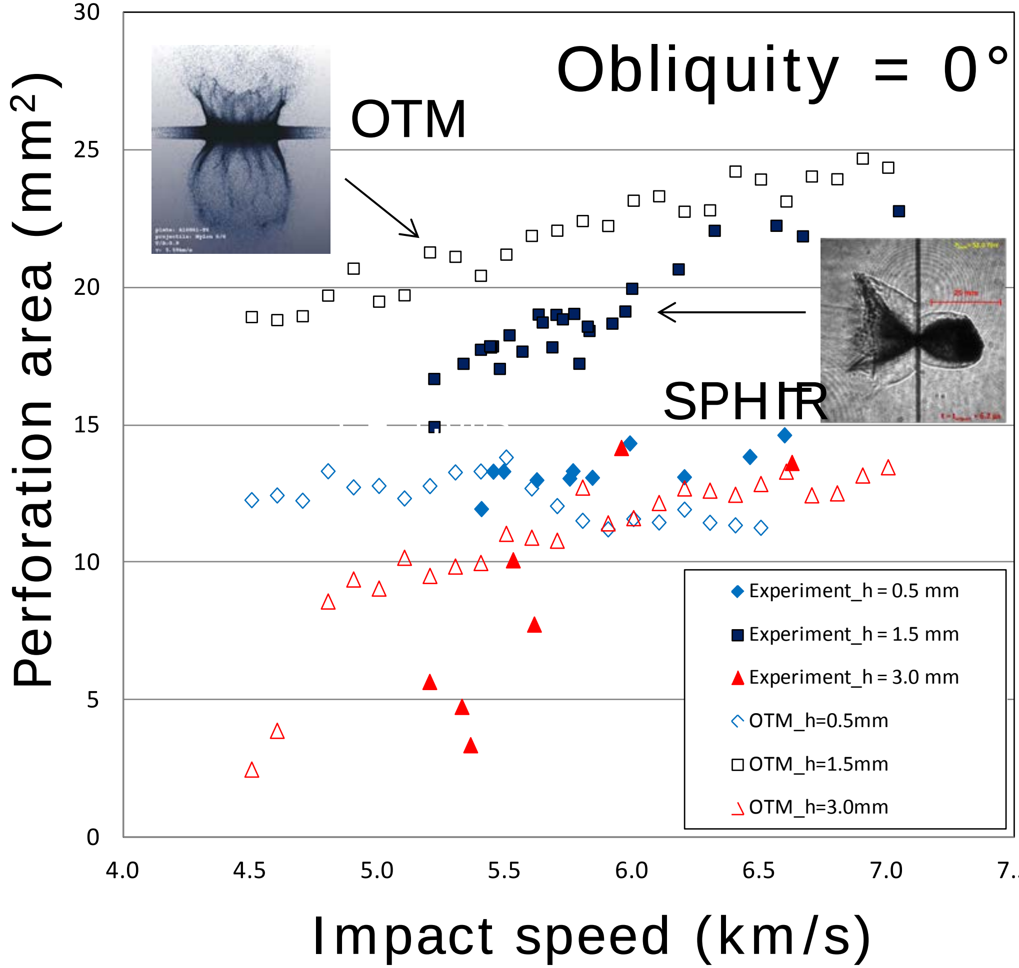

Mihaly, J.M., *et al.*, *Int. J. Impact Eng.*, **62** (2014) 13.

Li, B., Stalzer, M. & Ortiz, M., *IJNME* (2014) in press.

Taylor-anvil tests on polyurea

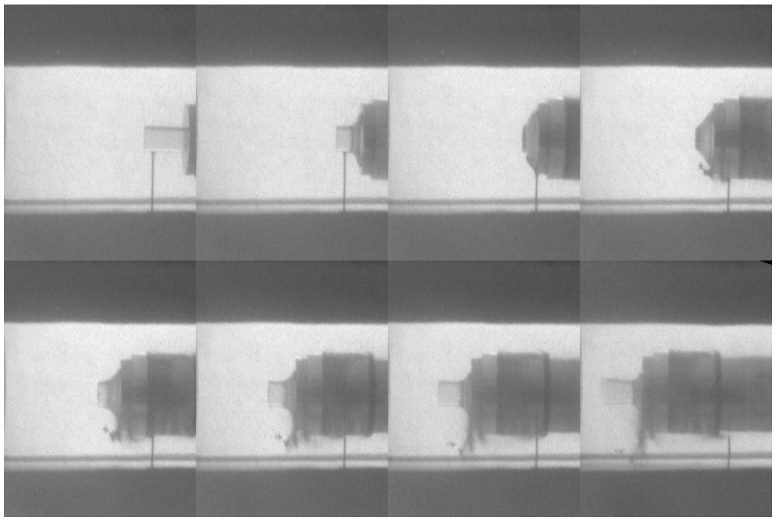

Shot #854:
R0 = 6.3075 mm,
L0 = 27.6897 mm,
v = 332 m/s

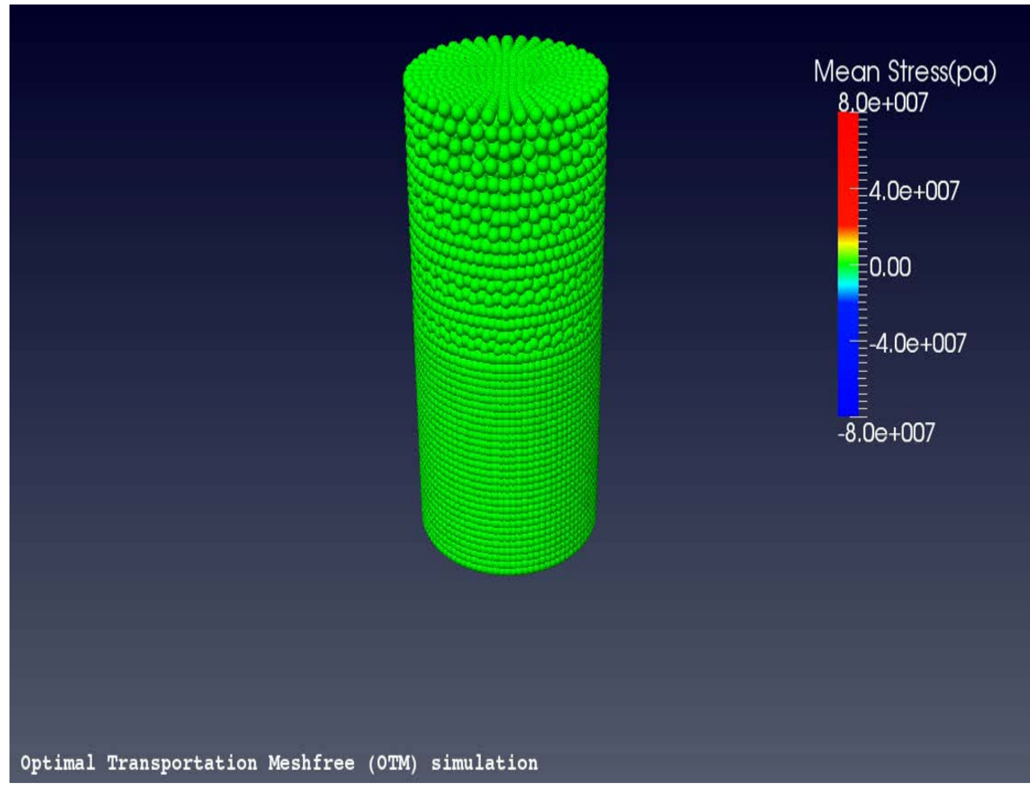

Experiments conducted by W. Mock, Jr. and J. Drotar,
at the Naval Surface Warfare Center (Dahlgren Division)
Research Gas Gun Facility, Dahlgren, VA 22448-5100, USA

Heyden, S. *et al.*, *JMPS* (2014) in press.

Experiments and simulations

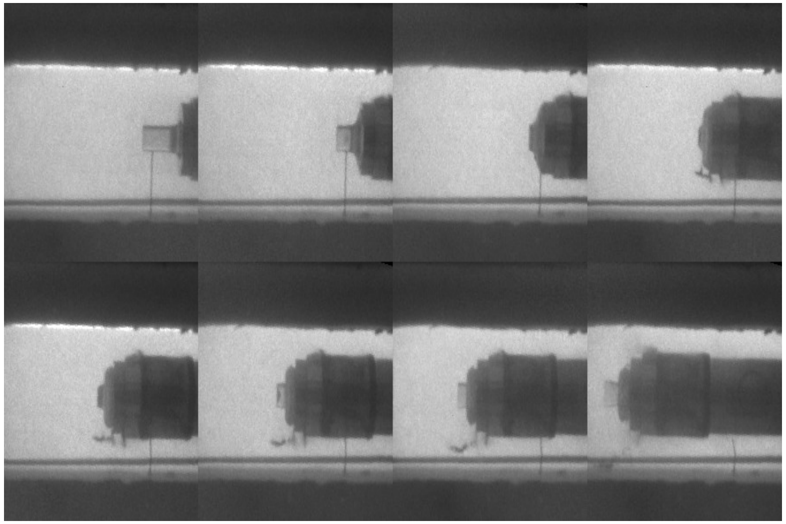

Shot #861:
R0 = 6.3039 mm,
L0 = 27.1698 mm,
v = 424 m/s

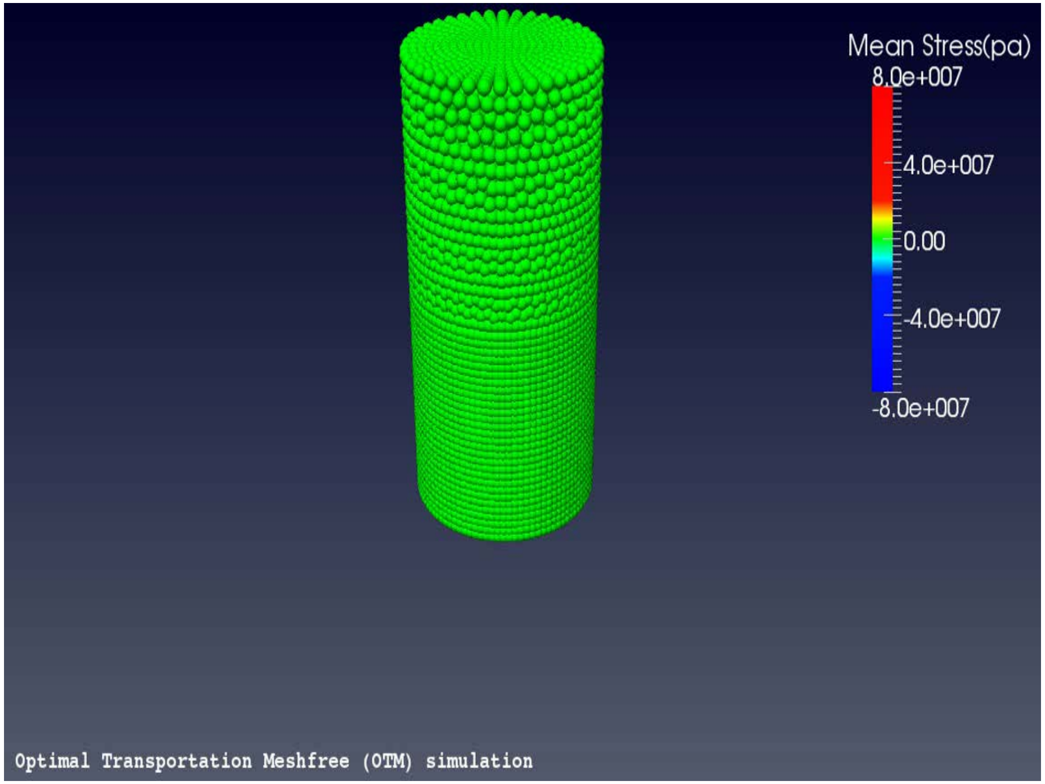

Experiments conducted by W. Mock, Jr. and J. Drotar,
at the Naval Surface Warfare Center (Dahlgren Division)
Research Gas Gun Facility, Dahlgren, VA 22448-5100, USA

Heyden, S. *et al.*, *JMPS* (2014) in press.

Taylor-anvil tests on polyurea

Shot #854

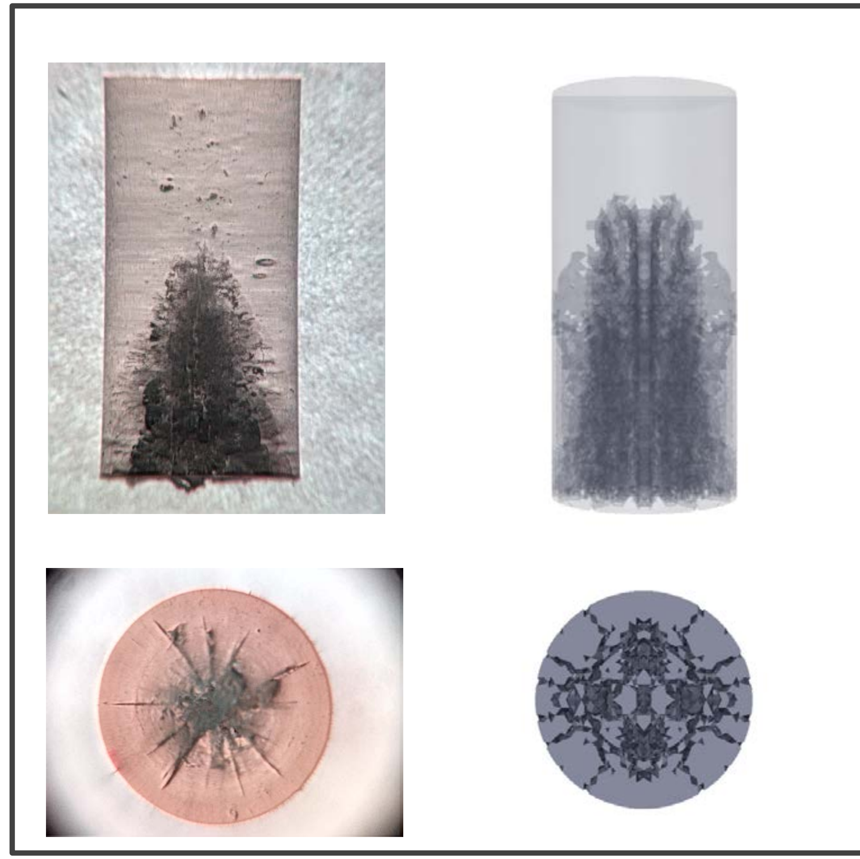

Shot #861

Comparison of damage and fracture patterns
in recovered specimens and simulations

Heyden, S. *et al.*, *JMPS* (2014) in press.

Michael Ortiz
WCCM XI

Concluding remarks

- Real-life fracture-dominated phenomena are often characterized by *complexity*, coupling to *inelastic/extreme material behavior*, coupling to *environment*, *stochasticity*, *uncertainty*...
- Successful/useful numerical schemes rise to these challenges by accounting for *complex fracture patterns*, *arbitrary material behavior*, *statics* and *dynamics*...
- Admissible approximation schemes must be *provably convergent* and *predictive*...
- Also important are *ease of implementation, computational efficiency*...

Thank you!